Project

Numerical Optimization

UGWONALI Nathan

Project initiated in L3 SAPHIRE at ENS Paris-Saclay
Resumed and expanded in M1 Mathematics and Applications at Sorbonne Université

Academic Year 2025–2026

1 Context and Definition of the Physical Problem

This work initially began as part of the L3 Optimization course (Prof. Kieffer) at ENS Paris-Saclay. It was later resumed, refactored, and expanded in light of the advanced mathematical concepts studied in the M1 Optimization course (Prof. Trélat) at Jussieu, Sorbonne Université.

The objective is to solve an inverse geophysical problem: detecting and characterizing an underground cavity (inclusion) using a single set of vertical surface displacement measurements (data comparable to radar interferometry).

The subsurface is modeled as a 2D semi-infinite elastic medium with dimensions of 100×100 meters. The elliptical cavity is characterized by four unknown parameters:

- x_c: lateral position (center)
- z_c: depth (center)
- a: semi-width
- b: semi-height

Neglecting Poisson's ratio effects, static mechanical equilibrium relates strain ϵ_z to displacement U_z through the integration of the fundamental relation:

$$E \frac{\partial \epsilon_z}{\partial z} + \rho g = 0 \tag{1}$$

2 The Forward Model

For a given set of parameters (x_c, z_c, a, b), the forward model computes the displacement field. The algorithmic implementation was heavily optimized via **matrix vectorization** (NumPy), eliminating iterative loops along the horizontal axis. This refactoring allows the surface displacement to be evaluated very rapidly, which is an essential condition for running stochastic optimization algorithms requiring thousands of evaluations.

3 Inverse Problem and Algorithmic Optimization

The inverse problem consists of minimizing the scalar cost function (L^2 norm of the residuals):

$$Cost(x_c, z_c, a, b) = \|U_z^{\text{computed}} - U_z^{\text{measured}}\|^2 \tag{2}$$

3.1 Limitations of Classical Approaches

The initial implementation (Gauss-Newton) revealed strong instabilities, with an extreme sensitivity to initial conditions leading to local minima. A classical optimal step gradient descent then showed its limitations in terms of slowness in areas where the cost function forms highly stretched "valleys".

3.2 Non-Linear Conjugate Gradient (Polak-Ribière) and Multi-Start

To overcome the ill-conditioning of the geophysical problem, a **non-linear Conjugate Gradient** method was developed. Unlike the classical gradient, this method retains a memory (inertia) of previous descent directions to accelerate convergence in narrow valleys.

The conjugate direction update is performed via the parameter β_k, calculated according to the **Polak-Ribière** formula, known for its robustness on non-convex functions:

$$\beta_k^{PR} = \frac{\nabla f(x_k)^T(\nabla f(x_k) - \nabla f(x_{k-1}))}{\|\nabla f(x_{k-1})\|^2} \tag{3}$$

Note: A restart condition $\beta_k = \max(0, \beta_k^{PR})$ *was implemented to guarantee a strict descent direction.*

To definitively overcome the problem of local minima identified on the cost surface, this algorithm was embedded in a **Multi-Start** strategy (physically constrained random starting points), making it possible to retain the best global minimum across all simulations.

4 Topological Analysis and Ill-Posed Problem

The 3D analysis of the cost function's contour lines highlighted the fundamental difficulty of the problem, corroborating observations from the literature regarding the identification of spatial fields of material properties.

- **Strong convergence (x_c, a)**: The gradient is very steep along the horizontal axis. The algorithm identifies the lateral position and width with high precision.
- **The equivalence valley (Depth z_c vs Height b)**: The cost function features a long "degenerate" valley. A deeper but taller inclusion generates a surface subsidence almost identical to a shallower and thinner inclusion. The algorithm quickly slides to the bottom of this valley but stagnates there due to gradients close to zero.
- **Discrete Locking**: The rigid rectangular mesh (1×1 m) causes constant error plateaus at the sub-pixel scale.

4.1 Convergence Analysis

Figure 1 illustrates the decrease in relative error over the iterations for the best starting point of the Multi-Start.

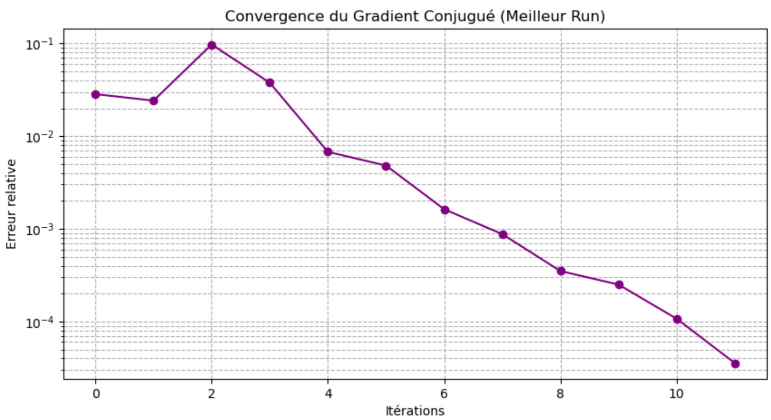

Figure 1: Evolution of the relative error (logarithmic scale) via the Conjugate Gradient (Polak-Ribière) algorithm.

The conjugate approach yields a stable and monotonic descent. The calculation of the Cauchy optimal step avoids the severe oscillations and divergences outside the physical domain that were frequent with the initial Gauss-Newton algorithm.

4.2 Geometric Reconstruction and Equivalence Principle

Figure 2 overlays the real cavity (target) and the cavity reconstructed by our algorithm.

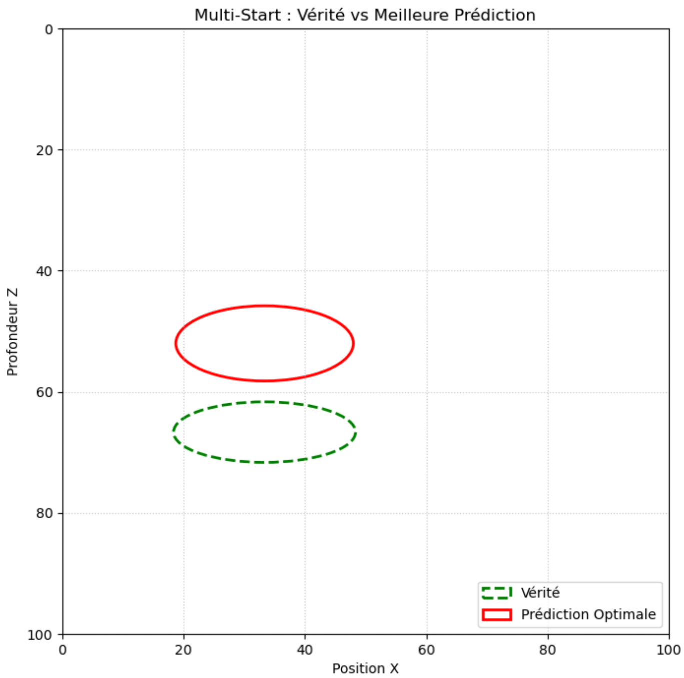

Figure 2: Spatial comparison between the real cavity (green dashed line) and the algorithm's prediction (solid red line).

The algorithm identifies the lateral position (x_c) and the width (a) with excellent precision, as the cost function's gradient is very steep along these axes. However, a slight offset is observed for the depth (z_c) and the height (b).

This behavior is not an algorithmic failure, but the manifestation of an **ill-posed** problem. To prove this, we plotted the contour lines of the cost function with respect to depth and height (Figure 3).

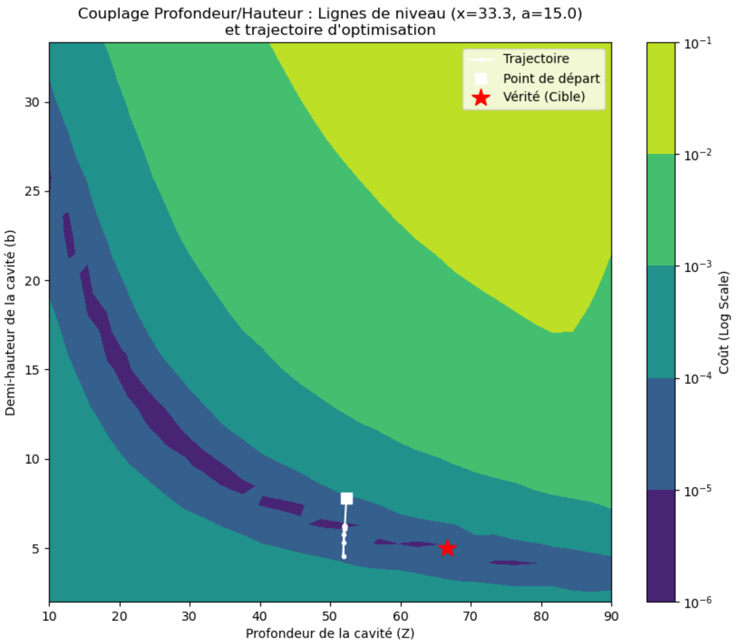

Figure 3: Cost function landscape (logarithmic scale) showing the "equivalence valley" between depth Z and height b, along with the optimization trajectory.

The analysis of this surface reveals a **degenerate equivalence valley** (in the shape of a diagonal corridor). Physically, this means that a deeper but taller inclusion generates a surface subsidence almost identical to a shallower and thinner inclusion. The algorithm quickly slides to the bottom of this valley (as illustrated by the trajectory) but ends up stagnating due to an almost zero gradient ($< 10^{-12}$).

5 Conclusion and Perspectives

The implementation of the Polak-Ribière Conjugate Gradient coupled with stochastic exploration (Multi-Start) successfully stabilized the inversion mathematically and reconstructed the cavity's geometry with high fidelity along its major axes.

However, the stagnation of the error in the "depth/height" equivalence valley illustrates the physical limits of an inversion based solely on vertical surface displacement. In accordance with the avenues suggested by G. Puel and D. Aubry [1], [2], an improvement would be to implement **dynamic mesh adaptation** around the inclusion's boundary to artificially smooth the cost function and break the discrete locking effects.

References

[1] Guillaume Puel and Denis Aubry. Using mesh adaption for the identification of a spatial field of material properties. *International Journal for Numerical Methods in Engineering*, 88(3):205–227, 2011.

[2] Guillaume Puel and Denis Aubry. Identification paramétrique de modèles à échelles de temps multiples. In *11e Colloque National en Calcul des Structures*, Giens, France, 2013.